An Extended-State-Observer-Based Sliding-Mode Speed Control for Permanent-Magnet Synchronous Motors

Lizhi Qu, *Member, IEEE*, Wei Qiao, *Fellow, IEEE*, and Liyan Qu, *Senior Member, IEEE*

***Abstract*— To improve the tracking performance of the speed controllers of permanent-magnet synchronous motor (PMSM) drive systems with different disturbances, such as internal parameter variations and external load changes, a novel extended-state-observer-based sliding-mode speed control (ESO-SMSC) scheme for PMSM drives is proposed in this article. First, a fast-response SMSC is designed based on the upper bound of the total disturbance. Then, an ESO is designed to estimate the total disturbance in real time. The parameters of the ESO can be easily designed based on the desired bandwidth of the ESO. The estimated total disturbance is then used to update the control law of the SMSC in real time. The resulting ESO-SMSC has improved speed tracking performance and strong robustness to disturbances while maintaining the fast dynamic response. The stability of the closed-loop PMSM drive system with the proposed ESO-SMSC is proven through the Lyapunov theory. The proposed ESO-SMSC is validated by experimental results for a 200-W salient-pole PMSM drive system.**

***Index Terms*— Active disturbance rejection control (ADRC), extended state observer (ESO), permanent-magnet synchronous motor (PMSM), sling-mode speed control (SMSC).**

I. Introduction

PERMANENT-MAGNET synchronous motor (PMSM) drives have been widely used in many industrial applications due to their high power density, high efficiency, and high reliability. The closed-loop control schemes of PMSM drives are commonly designed by using the field-oriented control (FOC) technique. If an FOC-based PMSM drive operates in a speed control mode, the outer-loop speed control provides the reference signal for the inner current loop and, therefore, affects the performance of the whole drive system directly. Due to its simplicity, the traditional linear proportional-integral (PI) control method has been widely applied to design the speed controllers for PMSM drives [1]. However, internal and external uncertain disturbances, such as parameter and load variations, respectively, are always present in practical PMSM drives. It is difficult to mitigate these disturbances rapidly when using the traditional linear PI controller.

To improve the performance of the PMSM drive systems with different uncertain disturbances, many advanced control schemes, such as adaptive control [2], intelligent control [3], predictive control [4], robust predictive control [5], and sliding-mode control (SMC), have been developed for the speed control of PMSM drives. Among these advanced control schemes, the SMC scheme has demonstrated superior tracking performance and robustness to internal parameter variations and external load disturbances in different applications [6], [7]. However, since it is hard to determine the upper bounds of the disturbances, the robustness of the SMC was usually achieved by using a large switching gain, which yielded an undesired chattering problem [8]. To overcome this drawback, combining the SMC with a disturbance observer is an attractive approach. The disturbance observer estimates the total disturbance of the system in real time, which is then compensated timely in the SMC to mitigate its impact [9], [10]. Various disturbance observers have been designed for the speed and current control of PMSM drives [11]–[14]. However, the design of these disturbance observers relied on an accurate model of the drive system.

Recently, the active disturbance rejection control (ADRC) method [15], [16], whose design does not require an accurate system model, has been applied for the disturbance-tolerant control of PMSM drives [17], [18]. In [17], a hybrid sensorless FOC scheme combining an ADRC-based high-frequency (HF) current injection method with another ADRC-based back electromotive force (EMF) method for the rotor position estimations in low- and high-speed regions, respectively, for PMSMs was presented. However, the speed loop was still designed by using the conventional PI controller. In [18], a linear ADRC (LADRC) combined with a load torque observer was proposed to realize a robust speed control for a five-phase PMSM to achieve a reduced overshoot and improved dynamic response when a disturbance occurred. The speed controller was designed by using the simple proportional control method.

This article proposes a novel extended-state-observer-based sliding-model speed controller (ESO-SMSC) for FOC-based PMSM drives to improve their disturbance rejection ability as

Manuscript received November 13, 2019; revised January 23, 2020 and March 30, 2020; accepted April 18, 2020. Date of publication April 27, 2020; date of current version April 1, 2021. This work was supported in part by the U.S. National Science Foundation under CAREER Award ECCS-1554497 and in part by the University of Nebraska Collaboration Initiative Seed Grant. Recommended for publication by Associate Editor Juan C. Balda. *(Corresponding authors: Wei Qiao; Liyan Qu.)*

Lizhi Qu is with Toshiba International Corporation, Houston, TX 77041 USA (e-mail: lizhi.qu@toshiba.com).

Wei Qiao and Liyan Qu are with the Power and Energy Systems Laboratory, Department of Electrical and Computer Engineering, University of Nebraska–Lincoln, Lincoln, NE 68588-0511 USA (e-mail: wqiao3@unl.edu; lqu2@unl.edu).

Color versions of one or more of the figures in this article are available online at https://ieeexplore.ieee.org.

Digital Object Identifier 10.1109/JESTPE.2020.2990442

well as steady-state and dynamic speed tracking performance. The disturbances considered include the rotor magnetic flux linkage and load torque variations. The ESO-SMSC combines an SMSC with an ESO, which is a core part of the ADRC. The SMSC is designed to achieve fast speed tracking performance based on the upper bound of the total disturbance, which is estimated in real time by the ESO whose parameter can be simply designed based on the desired bandwidth. The control law of the SMSC is then updated in real time by using the total disturbance estimated by the ESO in the feedforward path to mitigate the influence of the total disturbance on the speed tracking error in both steady-state and transient conditions. Thus, the proposed ESO-SMSC is robust to system disturbances and has fast speed tracking performance. The stability of the closed-loop PMSM drive system with the ESO-SMSC is proven by using the Lyapunov theory.

This article is organized as follows. Section II presents the dynamic motion model of a salient-pole PMSM without considering disturbance and the proposed SMSC. Section III presents the dynamic motion model of the PMSM considering disturbances, the proposed ESO and ESO-SMSC, the speed tracking error dynamic analysis, and the parameter tuning method for the ESO. Experimental results on a salient-pole PMSM drive system are provided in Section IV to show the superiority of the proposed ESO-SMSC over the conventional PI speed controller (PISC), the SMSC without using the ESO, and a disturbance observer-based SMSC (DO-SMSC) [9]. Finally, Section V provides concluding remarks of this article and a brief discussion of the future work.

II. Proposed SMSC for PMSM Drives

A. Dynamic Motion Model of a PMSM Without Considering Disturbance

The electromagnetic torque equation of a general salient-pole PMSM in the d-q reference frame is

$$T_e = \frac{3}{2} n_p [\psi_m i_{sq} + (L_d - L_q) i_{sd} i_{sq}] \tag{1}$$

where T_e is the electromagnetic torque; i_{sd} and i_{sq} are the d- and q-axis stator currents, respectively; L_d and L_q are the d- and q-axis inductances, respectively; ψ_m is the rotor magnet flux linkage; and n_p is the number of pole pairs.

The mechanical motion equation of the salient-pole PMSM can be written as

$$J \frac{d\omega_m}{dt} = T_e - T_L - B\omega_m \tag{2}$$

where J is the moment of inertia; B is the viscous friction coefficient; ω_m is the rotor mechanical angular speed; and T_L is the load torque.

In this article, the FOC system of the salient-pole PMSM uses the $i_{sd} = 0$ control method. Since $\omega_e = n_p \cdot \omega_m$, according to (1) and (2), the following equation can be obtained:

$$\begin{aligned} \frac{d\omega_e}{dt} &= \frac{1}{J}\left(\frac{3}{2} n_p^2 \psi_m i_{sq} - B\omega_e - n_p T_L\right) \\ &= a i_{sq} - b\omega_e - cT_L \end{aligned} \tag{3}$$

where $a = (3/2)(n_p^2 \psi_m / J)$, $b = (B/J)$, and $c = (n_p/J)$.

B. Proposed SMSC for the PMSM

Define the rotor speed error e_ω as follows:

$$e_\omega = \omega_e - \omega_{er} \tag{4}$$

where ω_{er} is the rotor speed reference. The objective of the SMSC is to control e_ω to be zero.

To design the SMSC, the following sliding surface function [7], [9], [19] is chosen due to its simple structure and precise steady-state speed tracking performance

$$\sigma_\omega = e_\omega + c_\omega \int e_\omega \tag{5}$$

where c_ω is a positive number that determines the decay rate of the rotor speed error.

Then, a suitable control law is derived such that σ_ω satisfies the following sliding mode condition:

$$\sigma_\omega \dot{\sigma}_\omega < 0. \tag{6}$$

If (6) is satisfied, σ_ω will approach zero in finite time. To satisfy (6), the control law of the SMSC can be designed as follows:

$$i_{sqr} = -\gamma \sigma_\omega - \eta \operatorname{sgn}(\sigma_\omega) \tag{7}$$

where i_{sqr} is the q-axis current reference; sgn is the sign function; γ is a positive number that determines the decay rate of the rotor speed error; η is the switching gain, which guarantees the stability, induces a sliding motion on the sliding surface in finite time, and is defined as follows:

$$\eta = \frac{1}{a}(b|\omega_e| + c\varphi_L + c_\omega |e_\omega|) \tag{8}$$

where φ_L is the bound of the absolute value of the load torque, i.e., $|T_L| < \varphi_L$. Then, the sliding mode condition (6) can be proven to be satisfied as follows:

$$\begin{aligned} \sigma_\omega \dot{\sigma}_\omega &= \sigma_\omega (a i_{sq} - b\omega_e - cT_L + c_\omega e_\omega) \\ &= -a\gamma \sigma_\omega^2 - a\eta \sigma_\omega \operatorname{sgn}(\sigma_\omega) + \sigma_\omega(-b\omega_e - cT_L + c_\omega e_\omega) \\ &\le -a\gamma \sigma_\omega^2 - a\eta |\sigma_\omega| + (b|\omega_e| + c\varphi_L + c_\omega |e_\omega|)|\sigma_\omega| \\ &= -a\gamma \sigma_\omega^2 < 0. \end{aligned} \tag{9}$$

Therefore, the closed-loop speed control system is asymptotically stable [20].

III. Proposed ESO-SMSC for PMSM Drives

A. Dynamic Motion Model of a PMSM Considering Disturbances

The SMSC has a certain degree of robustness to system disturbances, including parameter variations and external disturbances. To minimize the effect of the chattering problem, a small switching gain is desired for the SMSC. However, to ensure that the SMSC is robust to large disturbances, a large switching gain is desired, which, however, will lead to the undesired chattering problem. An attractive solution to this dilemma is to make the control law of the SMSC adaptive to the disturbances, which are estimated online by an observer.

To design an appropriate disturbance observer, the dynamic motion equation of the PMSM that considers machine parameter and load torque variations is expressed as follows according to (3):

$$\begin{aligned}\frac{d\omega_e}{dt} &= \frac{3}{2}\frac{n_p^2\psi_{m0}}{J_0}i_{\text{sq}} - \frac{B_0}{J_0}\omega_e + f_{\text{id}} + f_{\text{ed}}\\ &= a_0 i_{\text{sq}} - b_0\omega_e + f_{\text{id}} + f_{\text{ed}} \end{aligned} \tag{10}$$

where $a_0 = (3/2)(n_p^2\psi_{m0}/J_0)$; $b_0 = (B_0/J_0)$; the subscript "0" denotes nominal parameter values; f_{id} and f_{ed} represent the uncertain dynamics caused by machine parameter and external load torque variations, respectively, which are expressed as $f_{id} = -(\Delta J\dot{\omega}_e/J_0) - (\Delta B\omega_e/J_0) + (3/2)(n_p^2\Delta\psi_m i_{sq}/J_0)$ and $f_{\text{ed}} = -(n_p T_L/J_0)$, respectively, where $\Delta J = J - J_0$; $\Delta B = B - B_0$; $\Delta\psi_m = \psi_m - \psi_{m0}$; and J, B, and ψ_m are actual parameter values.

Let $f_{\text{td}} = f_{\text{id}} + f_{\text{ed}}$ be the total disturbance, $x = [\omega_e, f_{\text{td}}]^T$ be the state vector, and $u = [i_{\text{sq}}, 0]^T$ be the control input vector. Assume that f_{td} is constant during every sampling period. Then, the mathematical model (10) can be rewritten in the following matrix form:

$$\dot{x} = Ax + Bu \tag{11}$$

where

$$A = \begin{bmatrix} -\dfrac{B_0}{J_0} & 1 \\ 0 & 0 \end{bmatrix} \text{ and } B = \begin{bmatrix} \dfrac{3}{2}\dfrac{n_p^2\psi_{m0}}{J_0} & 0 \\ 0 & 0 \end{bmatrix}.$$

B. Proposed ESO-SMSC for the PMSM

An ESO is designed as follows to online estimate the total disturbance f_{td} for the speed control loop of the PMSM drive

$$\begin{cases} e_1 = \hat{\omega}_e - \omega_e \\ \dot{\hat{\omega}}_e = \hat{f}_{\text{td}} - \beta_{01}e_1 + a_0 i_{\text{sq}} - b_0\omega_e \\ \dot{\hat{f}}_{td} = -\beta_{02}e_1 \end{cases} \tag{12}$$

where $\hat{\omega}_e$ and $\hat{f}_{\text{td}}$ are the estimated values of ω_e and f_{td}, respectively; β_{01} and β_{02} are the gains of the ESO. Equations (12) indicate that the design of the ESO only requires the nominal values of the PMSM parameters and, thus, is robust to PMSM parameter variations.

By taking into account the estimated total disturbance, a new control law of the SMSC is designed as follows:

$$i_{\text{sqr}} = -\gamma\sigma_\omega - \eta'\text{sgn}(\sigma_\omega) - \frac{1}{a_0}\hat{f}_{\text{td}} \tag{13}$$

where $\eta' = \frac{1}{a_0}(b_0|\omega_e| + c_\omega|e_\omega|)$, which is much smaller than the original switching gain η expressed by (8) to avoid the chattering problem; and m is the compensation gain designed as $m = \sigma_\omega/\dot{\hat{f}}_{\text{td}} > 0$.

If the bandwidth of the ESO is high enough as compared with the time variation of the internal disturbance, the variation of f_{td} is nearly zero during each short sampling period, such as 100–200 μs commonly used for FOC-based PMSM drives, that is, $\dot{f}_{\text{td}} = 0$ [21]. Define the total disturbance observation error $\Delta f_{\text{td}} = f_{\text{td}} - \hat{f}_{\text{td}}$. Then

$$\Delta\dot{f}_{\text{td}} = \dot{f}_{\text{td}} - \dot{\hat{f}}_{\text{td}} = -\dot{\hat{f}}_{\text{td}}. \tag{14}$$

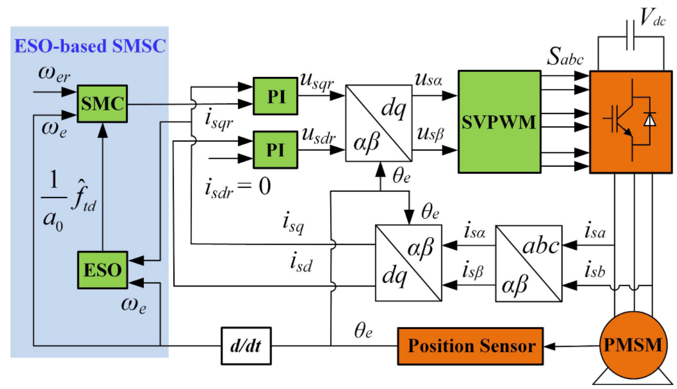

Fig. 1. Schematic of an FOC-based PMSM drive system with the proposed ESO-SMSC.

Define the following Lyapunov function:

$$V = \frac{1}{2}\sigma_\omega^2 + \frac{1}{2}m\Delta f_{\text{td}}^2. \tag{15}$$

Then, the derivative of V can be derived as follows:

$$\begin{aligned}\dot{V} &= \sigma_\omega\dot{\sigma}_\omega + m\Delta f_{td}\Delta\dot{f}_{td}\\ &= \sigma_\omega(a_0 i_{sq} - b_0\omega_e + f_{td} + c_\omega e_\omega) + m\Delta f_{td}\Delta\dot{f}_{td}\\ &= -a_0\gamma\sigma_\omega^2 - a_0\eta'\sigma_\omega\text{sgn}(\sigma_\omega) + \sigma_\omega(-b_0\omega_e + c_\omega e_\omega)\\ &\quad -m\Delta f_{td}\dot{\hat{f}}_{td} + \sigma_\omega\Delta f_{td}\\ &\le -a_0\gamma\sigma_\omega^2 - a_0\eta'|\sigma_\omega| + (b_0|\omega_e| + c_\omega|e_\omega|)|\sigma_\omega|\\ &\quad -m\Delta f_{td}\dot{\hat{f}}_{td} + \sigma_\omega\Delta f_{td}\\ &= -a_0\gamma\sigma_\omega^2 < 0. \end{aligned} \tag{16}$$

Thus, the asymptotical stability of the closed-loop speed control is proved. Finally, the proposed ESO-SMSC is obtained by combining (12) and (13).

Fig. 1 depicts the block diagram of the FOC-based PMSM drive using the proposed ESO-SMSC for the speed tracking control. The PMSM is fed by a pulse-width modulated (PWM) inverter. The entire control system adopts the commonly used double-loop structure. PI controllers are used for the inner current loop. The proposed ESO-SMSC is used for the outer speed loop, which generates the reference i_{sqr} for the torque producing current i_{sq}. The reference of the field current i_{sd} is set to be 0 A. An incremental encoder is used to measure the PMSM rotor speed ω_e. The rotor position θ_e is obtained by integrating the rotor speed ω_e for the coordinate transformation.

C. State Tracking Error Dynamics Analysis and Parameter Tuning Algorithm for the ESO

Equations (12) can be written in the following matrix form:

$$\dot{\hat{x}} = A_m\hat{x} + B_m u + C_m x \tag{17}$$

where $\hat{x} = [\hat{\omega}_e, \hat{f}_{td}]^T$ is the estimated state vector; A_m is the gain matrix of the ESO; and B_m and C_m are nominal matrices. These matrices are expressed as follows:

$$A_m = \begin{bmatrix} -\beta_{01} & 1 \\ -\beta_{02} & 0 \end{bmatrix}$$

$$B_m = B = \begin{bmatrix} \dfrac{3}{2}\dfrac{n_p^2\psi_{m0}}{J_0} & 0 \\ 0 & 0 \end{bmatrix}, \text{ and } C_m = \begin{bmatrix} -\frac{B_0}{J_0} + \beta_{01} & 0 \\ \beta_{02} & 0 \end{bmatrix}.$$

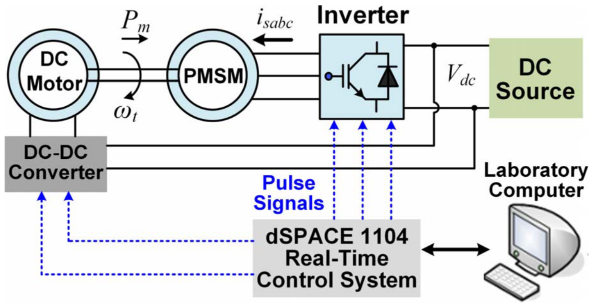

Fig. 2. Block diagram of the experiment system.

Subtracting (17) from (11) gives

$$\dot{e} = A_m e \tag{18}$$

where $e = [e_1,\ e_2]^T = [\hat{\omega}_e - \omega_e,\ \hat{f}_{td} - f_{td}]^T$. Equation (18) shows that the eigenvalues of A_m, which depend on the ESO parameters β_{01} and β_{02}, determine the behavior of the ESO. If and only if $\beta_{02} > 0$, the error dynamics (18) is asymptotically stable.

Since the state tracking error of the ESO is determined by the bandwidth of the ESO, i.e., the larger the bandwidth, the faster the tracking dynamics and, thus, the smaller the state tracking error, the parameters of the ESO can be simply designed according to the desired bandwidth of the ESO [16]. In this article, the parameters of the ESO are designed such that the matrix A_m has a double eigenvalue λ that is equal to the bandwidth of the ESO. Thus, the following equation should be satisfied:

$$|\lambda E - A_m| = \begin{vmatrix} \lambda + \beta_{01} & -1 \\ \beta_{02} & \lambda \end{vmatrix} = \lambda^2 + \beta_{01}\lambda + \beta_{02} = (\lambda - \omega_0)^2 \tag{19}$$

where ω_0 is viewed as the bandwidth of the ESO. Once ω_0 is chosen, the ESO parameters β_{01} and β_{02} can be determined according to (19) as $\beta_{01} = -2\omega_0$ and $\beta_{02} = \omega_0^2$. Thus, larger values of β_{01} and β_{02} lead to a larger bandwidth of the ESO.

The bandwidth ω_0 should be large enough to ensure that the dynamics of the ESO is sufficiently fast to track the variation of the total disturbance. On the other hand, a larger bandwidth will make the ESO more sensitive to sampling noise. Thus, in practice, the bandwidth of the ESO can be designed as a tradeoff between disturbance tracking performance and immunity to sampling noise.

IV. Experimental Results

A. Experiment Setup

Experimental studies are carried out for a 200-W FOC-based salient-pole PMSM drive system to evaluate the proposed ESO-SMSC in comparison with the conventional PISC, the SMSC, and the DO-SMSC [9]. The block diagram and hardware setup of the experiment system are shown in Figs. 2 and 3, respectively. The parameters of the PMSM are given as follows. The rated speed is 1500 rpm; the rated load torque is 1.5 N·m; the stator resistance is $R_s = 0.235\ \Omega$; the d-axis stator inductance is $L_d = 0.275$ mH; the q-axis stator inductance is $L_q = 0.364$ mH; the rotor magnet flux linkage is $\psi_{m0} = 0.013439$ V·s; the voltage constant is $K_e = 9.7$ mV/rpm; the number of pole pairs is $n_p = 4$; the moment of inertia is $J_0 = 0.000007$ kg·m^2; and the viscous friction coefficient is $B = 0.009$ N·m·s/rad. The DC bus voltage of the inverter is 41.75 V. The switching frequency of the inverter is 10 kHz. The control algorithms are implemented in a dSPACE 1104 real-time control system with a sampling period of 100 μs. The dead time was set as 1 μs.

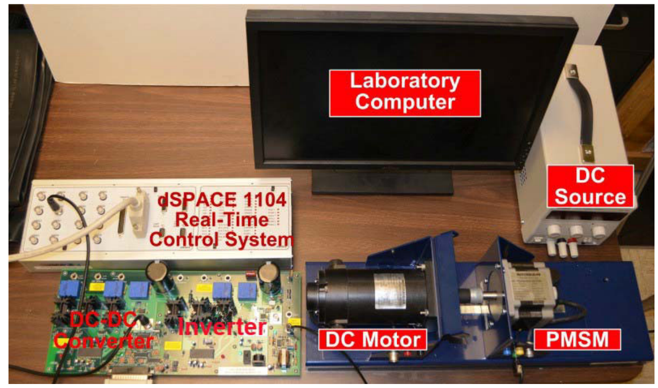

Fig. 3. Hardware setup of the experiment system.

TABLE I
PERFORMANCE COMPARISON OF THE FOUR SPEED CONTROLLERS UNDER SUDDEN SPEED CHANGES

Performance Metrics	ESO-SMSC	DO-SMSC	SMSC	PISC
Settling Time t_s (ms)	90	120	180	210
Rising Time t_r (ms)	82	115	130	170
Steady-State Tracking Error e_{ss} (rpm)	2	5	14	16

In the experimental studies, the parameters of the current loop are set to be the same for the PMSM drive with four different speed controllers. The bandwidth of the current loop PI controllers is selected as 2000 Hz. The bandwidth of the conventional PISC is chosen as 28.5 Hz according to [22] and [23]. The bandwidth of the ESO is designed as 90 Hz as a tradeoff between disturbance tracking performance and immunity to noise. The bandwidth of the DO of the DO-SMSC is the same as that of the ESO. The SMSC of the ESO-SMSC is the same as that of the DO-SMSC. The SMSC parameter γ that determines the decay rate of the rotor speed error is usually between 0 and 1 and is chosen to be 0.1 to achieve fast speed tracking performance in this article. The SMSC parameters η and η' are chosen to be 2 and 0.01 according to (8) and the definition after (13), respectively. The total compensation gain m/a_0, which only needs to be larger than zero, is chosen to be 0.5 as a tradeoff between steady-state and transient performance.

B. Sudden Speed Changes at Constant Load Torque Without Parameter Mismatch

In this test, the torque reference is kept constant at 1.5 N·m but the speed reference is step changed from 1000 to 1500 rpm and then back to 1000 rpm. Fig. 4 shows the comparison of the reference and actual rotor speeds and the rotor speed tracking errors of the PMSM with the PISC, the SMSC, the DO-SMSC, and the proposed ESO-SMSC during the test. Fig. 4 shows the comparison of the detailed transient responses

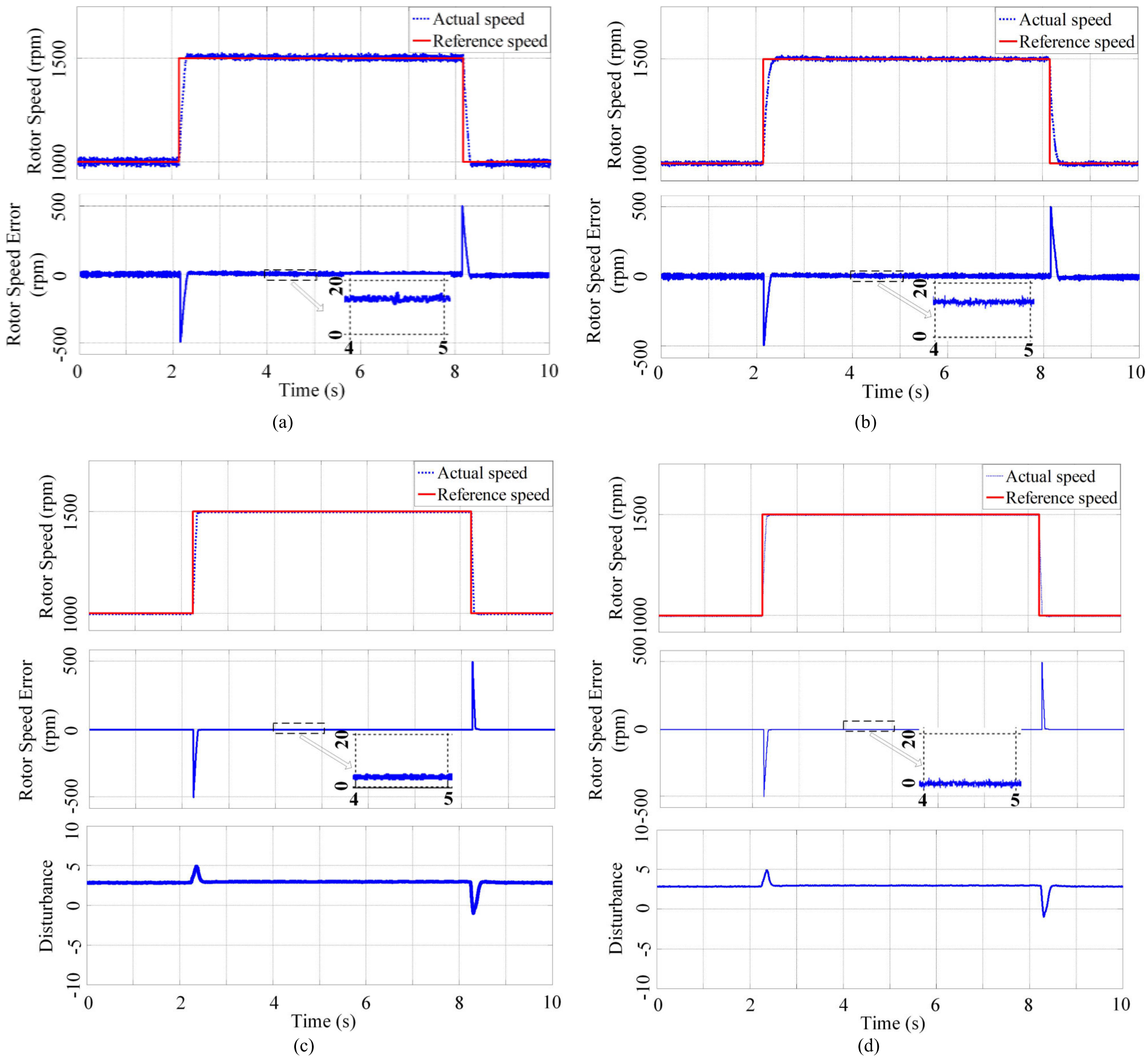

Fig. 4. Experimental results under sudden speed changes. (a) PISC. (b) SMSC. (c) DO-SMSC. (d) Proposed ESO-SMSC.

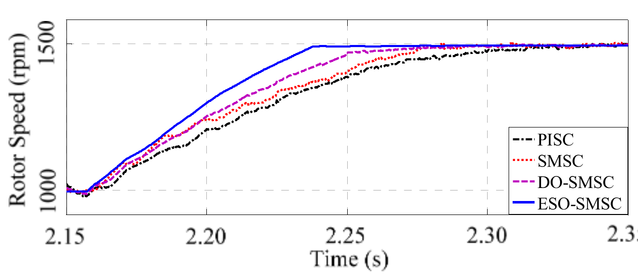

Fig. 5. Comparison of transient responses of the four speed controllers.

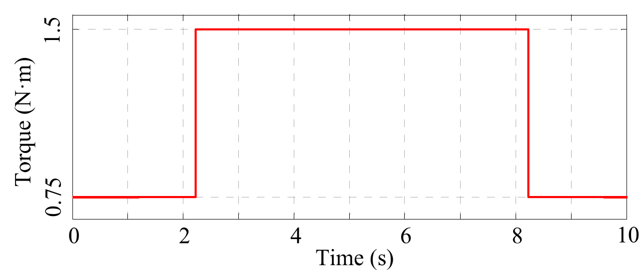

Fig. 6. Load torque reference for the four controllers.

of the four speed controllers. Table I provides the comparison of the settling time t_s, rising time t_r, and average steady-state tracking error e_{ss} of the PMSM rotor speed using the four speed controllers after the step changes in the speed command. The settling time and rising time of the proposed ESO-SMSC after the sudden speed changes are 90 and 82 ms, respectively, which are much shorter than 120 and 115 ms of the DO-SMSC, 180 and 130 ms of the SMSC, and 210 and 170 ms of the PISC, respectively. The speed rising times of the PMSM using the four different speed controllers are also clearly shown in Fig. 5. Moreover, the steady-state speed tracking error of the proposed ESO-SMSC is 2 rpm, which is much smaller than 5 rpm of the DO-SMSC, 14 rpm of the SMSC, and 16 rpm of the PISC. These results show that by properly estimating and compensating the total disturbance shown in Fig. 4(d), the ESO-SMSC has better steady-state

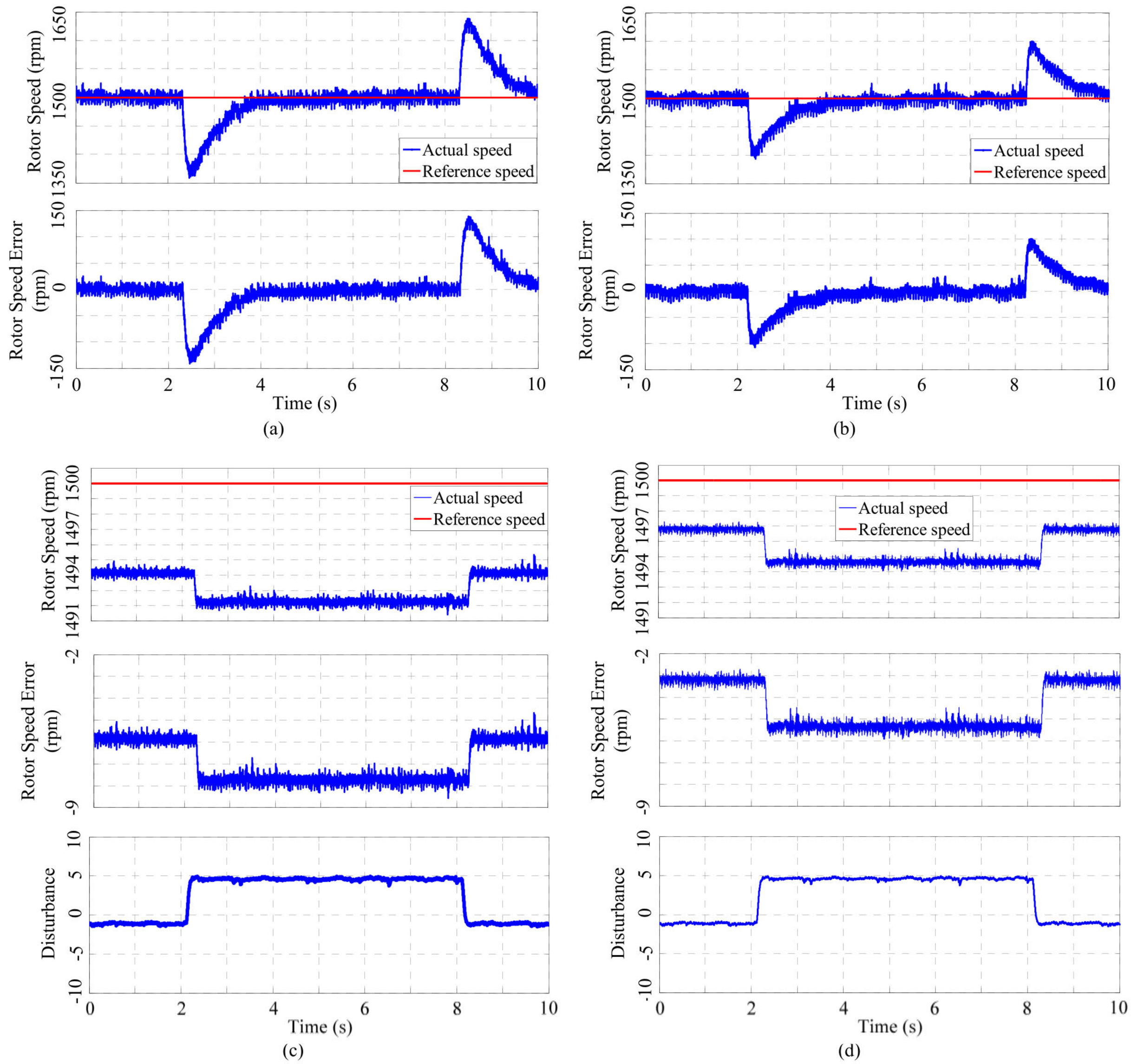

Fig. 7. Experimental results under sudden load torque changes. (a) PISC. (b) SMSC. (c) DO-SMSC. (d) Proposed ESO-SMSC.

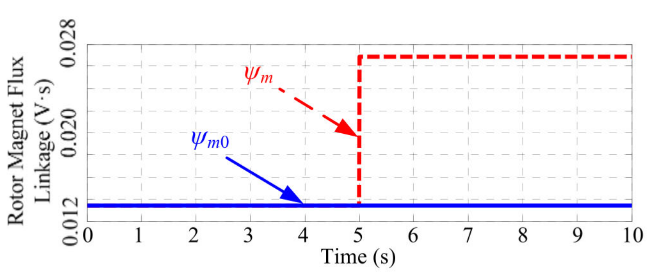

Fig. 8. Mismatch of the rotor magnetic flux linkage used by the five speed controllers.

and transient speed tracking performance than the PISC, the SMSC, and the DO-SMSC.

C. Sudden Load Torque Changes at Constant Speed Without Parameter Mismatch

In the second test, the load torque, which is an external disturbance, is step changed from 0.75 to 1.5 N·m and then back to 0.75 N·m, as shown in Fig. 6. The speed reference is kept constant at 1500 rpm during the test. Fig. 7 shows the comparison of the reference and actual rotor speeds and shows the rotor speed tracking errors of the PMSM with the PISC, the SMSC, the DO-SMSC, and the proposed ESO-SMSC during the test. Table II shows that the average steady-state tracking error e_{ss} of the PMSM rotor speed after the step changes in the load torque using the proposed ESO-SMSC is only 65.7%, 22%, and 20%, respectively, of that using the DO-SMSC, the PISC, and the SMSC. Moreover, as shown in Fig. 7 and Table II, when using the ESO-SMSC and DO-SMSC, the speed overshoots after the step load torque changes are negligible, but are much larger when using the SMSC and

TABLE II

PERFORMANCE COMPARISON OF THE FOUR SPEED CONTROLLERS UNDER SUDDEN LOAD TORQUE CHANGES

Performance Metrics	ESO -SMSC	DO -SMSC	SMSC	PISC
Steady-State Tracking Error e_{ss} (rpm)	4.4	6.7	20	22
Overshoot e_{os} (rpm)	0	0	100	125

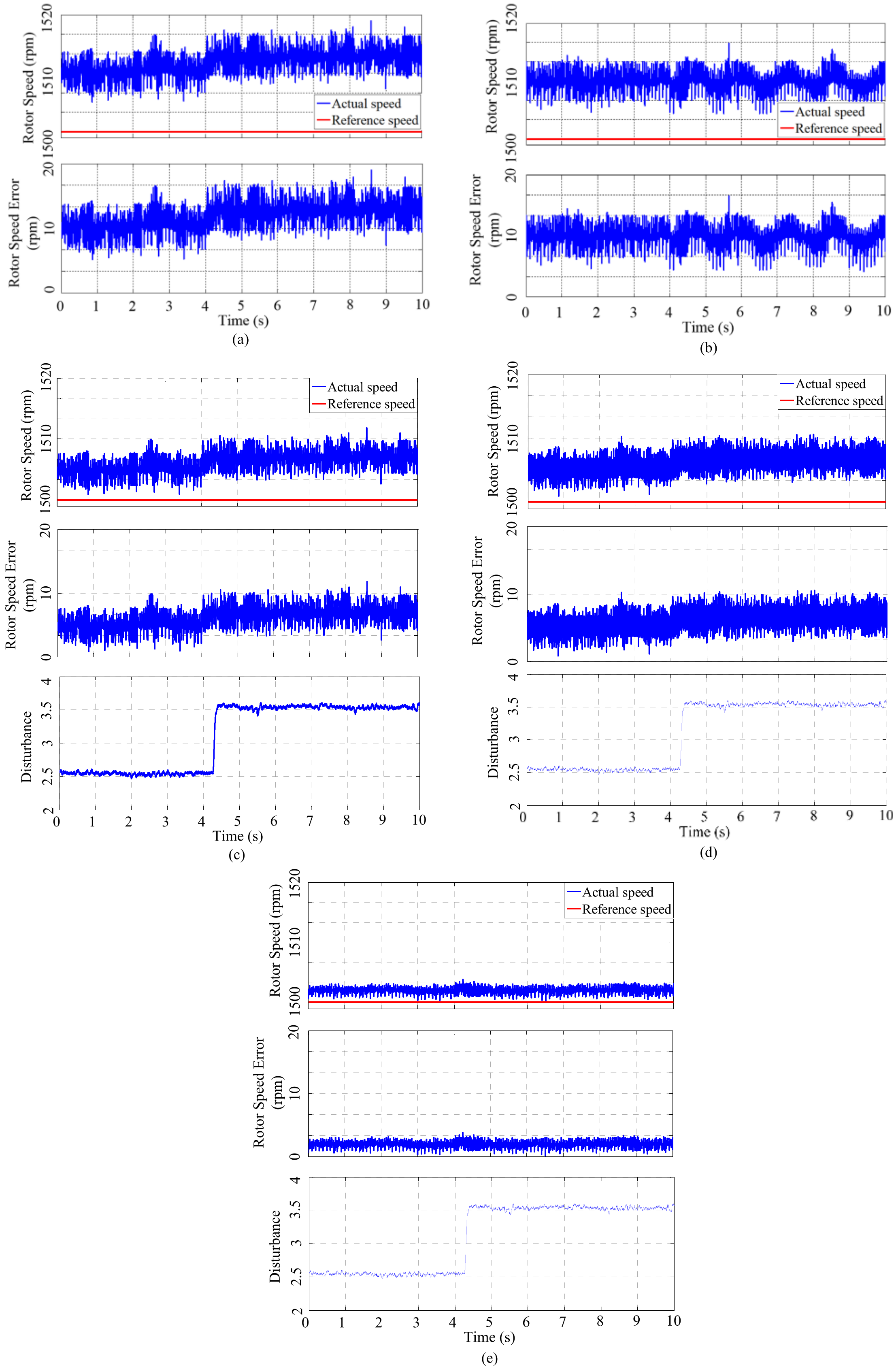

Fig. 9. Experimental results at 1500 rpm and the rated load with the rotor magnetic flux linkage mismatch. (a) PISC. (b) SMSC. (c) DO-SMSC. (d) ESO-PSC. (e) Proposed ESO-SMSC.

the largest when using the PISC. These results prove that by properly compensating the total disturbance $\hat{f}_{\text{td}}$ estimated by the ESO in real time, as shown in Fig. 7(d), the ESO-SMSC exhibits a remarkably improved capability of rejecting or

TABLE III
PERFORMANCE COMPARISON OF THE FIVE SPEED CONTROLLERS WITH PARAMETER MISMATCH

Performance Metrics	ESO-SMSC	ESO-PSC	DO-SMSC	SMSC	PISC
Steady-State Tracking Error e_{ss} (rpm) before Parameter Mismatch	2.5	4.9	5	11	13
Steady-State Tracking Error e_{ss} (rpm) after Parameter Mismatch	2.5	6.8	7	13	17

robustness to the external disturbance and, thus, has better steady-state and/or transient speed tracking performance than the conventional PISC, the SMSC, and the DO-SMSC.

D. Constant Load Torque and Constant Speed With Parameter Mismatch

In the third test, the robustness of the proposed ESO-SMSC to rotor magnetic flux linkage variation is verified in comparison with the PISC, the SMSC, the DO-SMSC, and an ADRC-based speed controller that consists of an ESO and a proportional speed control (ESO-PSC). The bandwidth of the PSC is the same as that of the PISC. The bandwidth of the ESO is the same as that of the proposed ESO-SMSC. The speed reference and load torque are kept constant at 1500 rpm and 1.5 N·m, respectively. Assume that the rotor magnetic flux linkage ψ_m used by the five speed controllers is mismeasured to be 200% of ψ_{m0} from 4.2 s onwards, as shown in Fig. 8. Fig. 9 and Table III shows the comparison of the rotor speed tracking performance of the PMSM using the five speed controllers during the test. The results clearly show that both the average value and the magnitude of oscillation of the steady-state tracking error of the PMSM rotor speed using the proposed ESO-SMSC are much smaller than those using the PISC, the SMSC, DO-SMSC, and the ESO-PSC. Moreover, with the help of the ESO to estimate and compensate the total disturbance $\hat{f}_{\mathrm{td}}$ in the ESO-SMSC, as shown in Fig. 9(e) and Table III, the rotor speed tracking performance is not affected by the parameter mismatch at all. However, when using the PISC, the SMSC, the DO-SMSC, or the ESO-PSC, the rotor speed tracking error increases when the parameter mismatch occurs. Therefore, the ESO-SMSC exhibits an improved capability of rejecting or robustness to internal disturbance (parameter mismatch) compared to the PISC, the SMSC, the DO-SMSC, and the ESO-PSC.

V. CONCLUSION

An ESO-SMSC was proposed for PMSM drive systems to achieve a fast dynamic response, precise tracking performance, and high robustness to disturbances of the system, such as parameter variations and load torque changes. First, a fast-response SMSC was designed based on the upper bound of the total disturbance. Then, an ESO was proposed to online estimate the total disturbance of the PMSM drive system. Finally, the control law of the SMSC was adapted by compensating the estimated total disturbance with the stability proven by the Lyapunov theory, leading to an ESO-SMSC with improved disturbance rejection ability over the SMSC. The experimental results showed that the PMSM drive system using the proposed ESO-based SMSC has a better disturbance rejection capability, smaller steady-state speed tracking error, and improved dynamic response than that using the conventional PISC, the SMSC, the DO-SMSC, and the ESO-PSC.

In the future work, the ESO-based SMC method will be applied to the current loop of the PMSM drive system to further improve the robustness of the closed-loop system to other disturbances such as inductance and/or resistance variations.

REFERENCES

[1] R. Sanchis, J. A. Romero, and P. Balaguer, “A simple procedure to design PID controllers in the frequency domain,” in *Proc. 35th Annu. Conf. IEEE Ind. Electron.*, Nov. 2009, pp. 1420–1425.

[2] X. Wang, B. Ufnalski, and L. M. Grzesiak, “Adaptive speed control in the PMSM drive for a non-stationary repetitive process using particle swarms,” in *Proc. 10th Int. Conf. Compat., Power Electron. Power Eng. (CPE-POWERENG)*, Jun. 2016, pp. 464–471.

[3] Y.-S. Kung and M.-H. Tsai, “FPGA-based speed control IC for PMSM drive with adaptive fuzzy control,” *IEEE Trans. Power Electron.*, vol. 22, no. 6, pp. 2476–2486, Nov. 2007.

[4] B. Bossoufi, H. A. Aroussi, M. El Ghamrasni, and Y. Ihedrane, “Speed control for PMSM drive system using predictive control,” in *Proc. 8th Int. Conf. Electron., Comput. Artif. Intell. (ECAI)*, Jun. 2016, pp. 1–6.

[5] T. Tarczewski and L. M. Grzesiak, “Constrained state feedback speed control of PMSM based on model predictive approach,” *IEEE Trans. Ind. Electron.*, vol. 63, no. 6, pp. 3867–3875, Jun. 2016.

[6] L. Wang, T. Chai, and L. Zhai, “Neural-network-based terminal sliding-mode control of robotic manipulators including actuator dynamics,” *IEEE Trans. Ind. Electron.*, vol. 56, no. 9, pp. 3296–3304, Sep. 2009.

[7] V. Q. Leu, H. H. Choi, and J.-W. Jung, “Fuzzy sliding mode speed controller for PM synchronous motors with a load torque observer,” *IEEE Trans. Power Electron.*, vol. 27, no. 3, pp. 1530–1539, Mar. 2012.

[8] K. D. Young, V. I. Utkin, and U. Ozguner, “A control engineer’s guide to sliding mode control,” *IEEE Trans. Control Syst. Technol.*, vol. 7, no. 3, pp. 328–342, May 1999.

[9] X. Zhang, L. Sun, K. Zhao, and L. Sun, “Nonlinear speed control for PMSM system using sliding-mode control and disturbance compensation techniques,” *IEEE Trans. Power Electron.*, vol. 28, no. 3, pp. 1358–1365, Mar. 2013.

[10] W.-H. Chen, J. Yang, L. Guo, and S. Li, “Disturbance-observer-based control and related methods—An overview,” *IEEE Trans. Ind. Electron.*, vol. 63, no. 2, pp. 1083–1095, Feb. 2016.

[11] W. Xu, Y. Jiang, and C. Mu, “Novel composite sliding mode control for PMSM drive system based on disturbance observer,” *IEEE Trans. Appl. Supercond.*, vol. 26, no. 7, pp. 1–5, Oct. 2016.

[12] J. Yang, W.-H. Chen, S. Li, L. Guo, and Y. Yan, “Disturbance/uncertainty estimation and attenuation techniques in PMSM drives—A survey,” *IEEE Trans. Ind. Electron.*, vol. 64, no. 4, pp. 3273–3285, Apr. 2017.

[13] J. Karttunen, S. Kallio, P. Peltoniemi, and P. Silventoinen, “Current harmonic compensation in dual three-phase PMSMs using a disturbance observer,” *IEEE Trans. Ind. Electron.*, vol. 63, no. 1, pp. 583–594, Jan. 2016.

[14] Y. A.-R.-I. Mohamed, “Design and implementation of a robust current-control scheme for a PMSM vector drive with a simple adaptive disturbance observer,” *IEEE Trans. Ind. Electron.*, vol. 54, no. 4, pp. 1981–1988, Aug. 2007.

[15] J. Han, “From PID to active disturbance rejection control,” *IEEE Trans. Ind. Electron.*, vol. 56, no. 3, pp. 900–906, Mar. 2009.

[16] Z. Gao, “Scaling and bandwidth-parameterization based controller tuning,” in *Proc. Amer. Control Conf.*, Jun. 2003, pp. 4989–4996.

[17] B. Du, S. Wu, S. Han, and S. Cui, “Application of linear active disturbance rejection controller for sensorless control of internal permanent-magnet synchronous motor,” *IEEE Trans. Ind. Electron.*, vol. 63, no. 5, pp. 3019–3027, May 2016.

[18] Z. Kuang, B. Du, S. Cui, and C. C. Chan, “Speed control of load torque feedforward compensation based on linear active disturbance rejection for five-phase PMSM,” *IEEE Access*, vol. 7, pp. 159787–159796, 2019.

[19] S. Li, M. Zhou, and X. Yu, “Design and implementation of terminal sliding mode control method for PMSM speed regulation system,” *IEEE Trans. Ind. Informat.*, vol. 9, no. 4, pp. 1879–1891, Nov. 2013.

[20] V. Utkin, J. Guldner, and J. Shi, *Sliding Mode Control in Electromechanical Systems*. New York, NY, USA: Taylor & Francis, 1999.

[21] K.-H. Kim, I.-C. Baik, G.-W. Moon, and M.-J. Youn, “A current control for a permanent magnet synchronous motor with a simple disturbance estimation scheme,” *IEEE Trans. Control Syst. Technol.*, vol. 7, no. 5, pp. 630–633, Sep. 1999.

[22] K. J. Astrom and T. Hagglund, *Advanced PID Control*. Research Triangle Park, NC, USA: ISA, 2006.

[23] K. J. Astrom and B. Witternmark, *Computer-Controlled Systems-Theory and Design*. Englewood Cliffs, NJ, USA: Prentice-Hall, 1990.

Lizhi Qu (Member, IEEE) received the B.Eng. and M.Eng. degrees in electrical engineering from the Harbin Institute of Technology, Harbin, China, in 2013 and 2015, respectively, and the Ph.D. degree in electrical engineering from the University of Nebraska−Lincoln, Lincoln, NE, USA, in 2019.

He worked as an Electrical Engineering Intern at Ford Motor Company, Dearborn, MI, USA, in summer 2018. He is currently a Software Development Engineer II with the Toshiba International Corporation, Houston, TX, USA. His research interests include power electronics and electric motor drives.

Wei Qiao (Fellow, IEEE) received the B.Eng. and M.Eng. degrees in electrical engineering from Zhejiang University, Hangzhou, China, in 1997 and 2002, respectively, the M.S. degree in high-performance computation for engineered systems from Singapore-MIT Alliance, Singapore, in 2003, and the Ph.D. degree in electrical engineering from the Georgia Institute of Technology, Atlanta, GA, USA, in 2008.

Since August 2008, he has been with the University of Nebraska–Lincoln, Lincoln, NE, USA, where he is currently a Professor with the Department of Electrical and Computer Engineering. He has authored or coauthored more than 250 articles in refereed journals and conference proceedings and holds ten U.S. patents issued. His research interests include renewable energy systems, smart grids, condition monitoring, power electronics, electric motor drives, energy storage systems, and emerging electrical energy conversion devices.

Dr. Qiao was a recipient of the 2010 U.S. National Science Foundation CAREER Award and the recipient of the 2010 IEEE Industry Applications Society Andrew W. Smith Outstanding Young Member Award. He is an Editor of the IEEE TRANSACTIONS ON ENERGY CONVERSION and an Associate Editor of the IEEE TRANSACTIONS ON POWER ELECTRONICS and the IEEE JOURNAL OF EMERGING AND SELECTED TOPICS IN POWER ELECTRONICS.

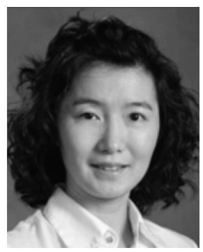

Liyan Qu (Senior Member, IEEE) received the B.Eng. (with highest distinction) and M.Eng. degrees in electrical engineering from Zhejiang University, Hangzhou, China, in 1999 and 2002, respectively, and the Ph.D. degree in electrical engineering from the University of Illinois at Urbana–Champaign, Champaign, IL, USA, in 2007.

From 2007 to 2009, she was an Application Engineer with Ansoft Corporation, Irvine, CA, USA. Since January 2010, she has been with the University of Nebraska−Lincoln, Lincoln, NE, USA, where she is currently an Associate Professor with the Department of Electrical and Computer Engineering. Her research interests include energy efficiency, renewable energy, numerical analysis and computer aided design of electric machinery and power electronic devices, dynamics and control of electric machinery, and magnetic devices.

Dr. Qu was a recipient of the 2016 U.S. National Science Foundation CAREER Award.